Isolation by crystallization of translational isomers of a bistable donor-acceptor [2]catenane

Cheng Wang[a,1], Mark A. Olson[a,1], Lei Fang[a], Diego Benítez[b], Ekaterina Tkatchouk[b], Subhadeep Basu[a], Ashish N. Basuray[a], Deqing Zhang[c], Daoben Zhu[c], William A. Goddard[b], and J. Fraser Stoddart[a,2]

[a]Department of Chemistry, Northwestern University, Evanston, IL 60208; [b]Materials and Process Simulation Center, California Institute of Technology, Pasadena, CA 91125; and [c]Beijing National Laboratory for Molecular Sciences, Organic Solids Laboratory, Institute of Chemistry, Chinese Academy of Sciences, Beijing 100190, China

Communicated by M. Frederick Hawthorne, University of Missouri, Columbia, MO, June 29, 2010 (received for review April 21, 2010)

The template-directed synthesis of a bistable donor-acceptor [2]catenane wherein both translational isomers—one in which a tetrathiafulvalene unit in a mechanically interlocked crown ether occupies the cavity of a cyclobis(paraquat-*p*-phenylene) ring and the other in which a 1,5-dioxynaphthalene unit in the crown ether resides inside the cavity of the tetracationic cyclophane—exist in equilibrium in solution, has led to the isolation and separation by hand picking of single crystals colored red and green, respectively. These two crystalline co-conformations have been characterized separately at both the molecular and supramolecular levels, and also by dynamic NMR spectroscopy in solution where there is compelling evidence that the mechanically interlocked molecules are present as a complex mixture of translational, configurational, and conformational isomers wherein the isomerization is best described as being a highly dynamic and adaptable phenomenon.

mechanical bond formation | stereochemistry | template-directed synthesis | structural isomerism | X-ray crystallography

The dynamics and stereochemical behavior of mechanically interlocked molecules (1–3) (MIMs) in solution require a fundamental understanding of the tenets of stereochemistry that reach beyond (4, 5) the commoner garden stereogenic centers that are normally how stereochemistry expresses itself—usually in a kinetically stable fashion—in organic compounds. In the 1980s Schill et al. (6) drew attention to the existence of translational isomerism (7–14) in catenanes and rotaxanes (15, 16). Subsequently, we proposed (17, 18) the use of the term co-conformation to describe different relative spatial arrangements of the components in MIMs—such as bistable [2]catenanes and [2]rotaxanes—in the context of molecular electronic devices (MEDs) (19). The reason we coined this variant of the term conformation is that the translational isomers of catenanes and rotaxanes are frequently (4, 5) separated by free energies of activation in the range of 8–24 kcal mol^{-1}—that is, the magnitudes of free energy barriers we associate with NMR observable conformational changes and isomerism over the experimentally accessible range of temperatures on commercially available spectrometers.

Whereas translational isomerism has some of the structural hallmarks (e.g., observable changes in shape and obvious alterations in structure) of conformational isomerism, and bears some superficial resemblance to it, it is not strictly correct—in the light of generally accepted definitions (20)—to refer to the relative movements between mechanically interlocked components in MIMs as a change in conformation. The reason is that the widely recognized definition (21) of the term conformation is as follows: The conformations of a molecule of defined configuration are the various arrangements of its atoms in space that differ only as after rotation about single bonds. This definition is now commonly extended to include rotation about π-bonds or bonds of partial order between one and two. Translational isomerism does not fall under this umbrella: hence, our introduction (17, 18) of the term co-conformation to describe a particular kind of translational isomerism that is observable using dynamic NMR spectroscopy (22). Just as dynamic NMR spectroscopy was employed (23, 24) in the 1960s to probe the equilibration of conformational diastereoisomers; e.g., the axial and equatorial isomers of chlorocyclohexane (25) and to study the conformational behavior of medium-sized ring compounds (26) in the 1980s, it has become possible, during the past decade, to investigate co-conformational equilibria in bistable donor-acceptor [2]catenanes (27) and [2]rotaxanes (28–30). The first really robust and efficient switchable [2]catenane (27) incorporating a tetrathiafulvalene (TTF) unit and a 1,5-dioxynaphthalene (DNP) one was employed subsequently to good effect in molecular switch tunnel junctions (MSTJs) in two-dimensional molecular electronic devices (2D MEDs) with crossbar architectures (31, 32). On account of the much stronger binding (33) of TTF to cyclobis(paraquat-*p*-phenylene) ($CBPQT^{4+}$) compared with DNP, the bistable [2]catenane (Fig. 1) exists preferentially (>9:1) as the translational isomer in which the TTF unit is included inside the $CBPQT^{4+}$ ring in the so-called (34) ground-state co-conformation (GSCC) rather than in the metastable state co-conformation (MSCC) where the DNP unit occupies the cavity inside the $CBPQT^{4+}$ ring. Oxidation of the TTF unit, however, alters the GSCC: MSCC exclusively in favor of the DNP unit residing inside the cavity of the $CBPQT^{4+}$ ring. To date, however, we have not been able to isolate and characterize the MSCC. The same scenario holds true for many (28–30) but not all (35, 36) the bistable [2]rotaxanes that have been designed and synthesized for incorporation (37, 38) into MSTJs in 2D MEDs, and more recently at metal (39, 40) nanoparticle and silica (41, 42) nanoparticle-solvent interfaces.

Here we report on (*i*) the design of a TTF/DNP/$CBPQT^{4+}$-[2]catenane that adopts both co-conformations in almost equal proportions in solution, (*ii*) the template-directed synthesis of this bistable donor-acceptor [2]catenane, (*iii*) its characterization by UV/Vis and ^{1}H NMR spectroscopies, as well as by electrochemical methods, (*iv*) crystallization of the [2]catenane in MeCN-$i\,Pr_2\,O$ and the manual separation of two crystalline forms—both rhomboidal in shape, with one set of single crystals colored red and the other green—which were examined separately by X-ray crystallography, (*v*) the outcome of computational studies performed on the two translational isomers identified in the solid state, and (*vi*) the measurement of the relaxation of one of the

Author contributions: C.W., M.A.O., L.F., and J.F.S. designed research; C.W., M.A.O., L.F., S.B., and A.N.B. performed research; D.B., E.T., D. Zhang, D. Zhu, and W.A.G. contributed new reagents/analytic tools; C.W., M.A.O., L.F., and J.F.S. analyzed data; and C.W., M.A.O., L.F. and J.F.S. wrote the paper.

The authors declare no conflict of interest.

Data deposition: Crystallographic data (excluding structure factors) for the structures have been deposited in the Cambridge Structural Database, Cambridge Crystallographic Data Centre, www.ccdc.cam.ac.uk/, Cambridge CB2 1EZ, United Kingdom (CSD reference nos. 782651 and 782652).

[1]C.W. and M.A.O. contributed equally to this work.

[2]To whom correspondence should be addressed. E-mail: stoddart@northwestern.edu.

This article contains supporting information online at www.pnas.org/lookup/suppl/doi:10.1073/pnas.1009302107/-/DCSupplemental.

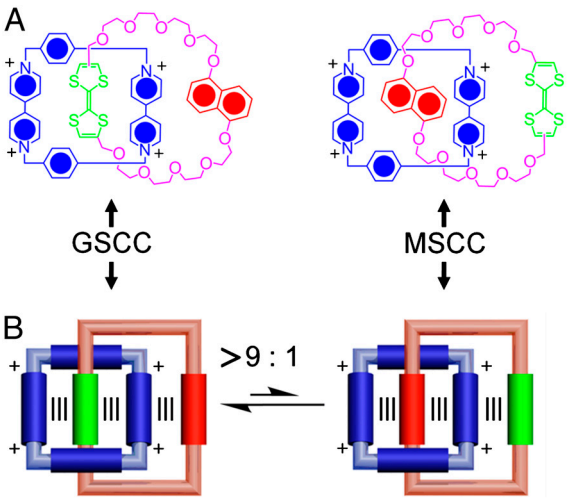

Fig. 1. (*A*) Structural formulas of the two translational isomers with different co-conformations—the ground state co-conformation (GSCC) and the metastable state co-conformation (MSCC)—of the first bistable [2]catenane to be obtained by template-directed synthesis. (*B*) The graphical representations of the GSCC and MSCC, illustrating the fact that the former is preferred over the latter in solution by greater than a 9 : 1 ratio. This predominance of one translational isomer over the other is in sharp contrast to $\mathbf{1}^{4+}$ where $\mathbf{1R}^{4+}$ and $\mathbf{1G}^{4+}$ are present in approximately equimolar amounts in solution.

translational isomers to an equilibrium mixture of both. It transpires that the mechanically interlocked molecules of the bistable [2]catenane populate the solution as a complex mixture of six enantiomeric pairs of translational, configurational, and conformational isomers from which two of the enantiomeric forms crystallize as one translational isomer where the TTF unit is located outside the $CBPQT^{4+}$ ring and adopts the *cis* configuration whereas the other translational isomer, where the TTF unit is located inside the $CBPQT^{4+}$ ring, adopts the *trans* configuration.

Results and Discussion

The bistable [2]catenane $\mathbf{1} \cdot 4PF_6$, whose template-directed synthesis is summarized in Fig. 2, and outlined in *Materials and Methods* is composed of a π-electron-deficient $CBPQT^{4+}$ ring and a crown ether containing two different π-electron-rich recognition sites. Investigation of the difference (34) in the free energies of binding ($\Delta\Delta G°$) between the two recognition sites present in $\mathbf{1} \cdot 4PF_6$—namely, 4,4′,(5′)-bis[2-(2-(2-(2-hydroxyethoxy)-ethoxy)ethoxy)ethylthio]tetrathiafulvalene (43, 44) (STTFS-TEG) and 1,5-bis[2-(2-(2-(2-hydroxyethoxy)ethoxy) ethoxy)ethoxy]-naphthalene (45) (DNP-TEG)—with the tetracationic receptor $CBPQT^{4+}$ by isothermal titration microcalorimetry indicates that the STTFS unit binds (*SI Appendix*) slightly more weakly to $CBPQT^{4+}$ than does the tetracationic cyclophane to the DNP unit. Because the $\Delta\Delta G°$ value comparing these two binding events is in the range of less than 1.0 kcal mol^{-1} (*SI Appendix*), the two co-conformations of $\mathbf{1} \cdot 4PF_6$ are expected to be present in roughly equal concentrations at room temperature: In $\mathbf{1R} \cdot 4PF_6$ the $CBPQT^{4+}$ ring encircles the STTFS unit and in $\mathbf{1G} \cdot 4PF_6$ the $CBPQT^{4+}$ ring encircles DNP unit. These two translational isomers are both stabilized by the π-electron donor–acceptor interactions between the $CBPQT^{4+}$ rings and the STTFS/DNP units, as well as by [C – H···O] interactions (7) between the oxygen atoms in the polyether loops of the crown ether and the hydrogen atoms on carbons α to nitrogen on the $CBPQT^{4+}$ ring.

To understand rather better the implications of replacing the TTF unit by a STTFS unit in bistable donor-acceptor [2]catenanes containing the $CBPQT^{4+}$ ring, we turned to density functional theory. Previously, we had shown (46) that the M06-suite of density functionals, especially the M06-L and the M06-HF variants, are a good choice for investigating (47) MIMs. The M06-L functional is adequate for geometry optimization in view of its reasonably good accuracy and relatively low cost—no Hartree–Fock exchange—whereas the M06-HF functional is a hybrid meta-GGA (generalized gradient approximation) with full Hartree–Fock exchange, especially accurate for long-range charge transfer (CT) and noncovalent bonding interactions. We used the M06-L functional in the gas phase to minimize both translational isomers $\mathbf{1R} \cdot 4PF_6$ and $\mathbf{1G} \cdot 4PF_6$ of $\mathbf{1} \cdot 4PF_6$ and the GSCC and MSCC of the bistable [2]catenane shown in Fig. 1*A*. We then calculated natural orbital populations (48) from the M06-HF wave functions. Natural populations show a +0.1 *e* charge difference for TTF when it is encircled by a $CBPQT^{4+}$ ring than when DNP is encircled by the tetracationic cyclophane. By contrast, in the case of $\mathbf{1} \cdot 4PF_6$, the difference in natural populations is 10 times smaller (+0.01 *e*). This difference reveals that the tetrathiafulvalene moiety in the STTFS unit has a virtually identical electronic population when it is encircled by a $CBPQT^{4+}$ ring than when it is not. However, when encircled by a $CBPQT^{4+}$ ring, the DNP unit has a very similar electronic population in both the bistable [2]catenanes—the one containing TTF (Fig. 1*A*) and $\mathbf{1} \cdot 4PF_6$. Additionally, our calculations reveal higher positive charges on the distal S atoms in STTFS, which in turn, reduces the ability to induce attractive [$\pi\cdots\pi$] stacking inside the tetracationic cyclophane in comparison with TTF. This observation could be interpreted as a "charge leak" that reduces the strength of the interaction.

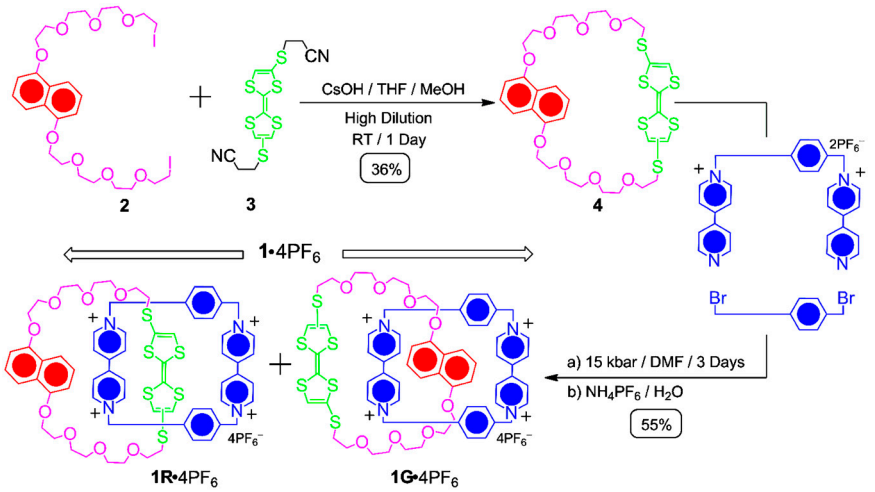

Fig. 2. The template-directed synthesis of the [2]catenane $\mathbf{1} \cdot 4PF_6$ in which the crown ether **4**—obtained from **2** and **3** under high dilution reaction conditions in the presence of CsOH—acts as the template for the formation of the catenated $CBPQT^{4+}$ ring. Spectroscopic evidence indicates that the [2]catenane exists in solution as an approximately equimolar mixture of the two translational isomers, $\mathbf{1R} \cdot 4PF_6$ and $\mathbf{1G} \cdot 4PF_6$.

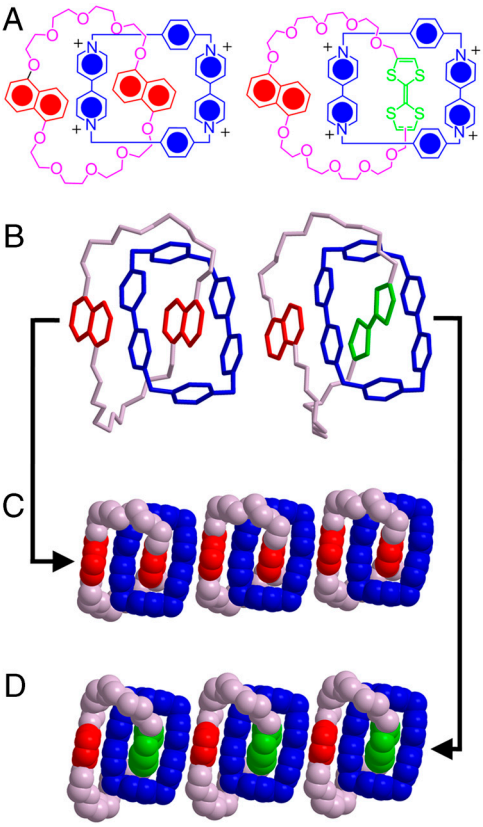

Fig. 3. (*A*) Structural formulas of the degenerate donor-acceptor [2]catenane containing two DNP units in its crown ether component, as well as of the bistable donor-acceptor [2]catenane mentioned in Fig. 1. It contains both a DNP and a TTF unit in its crown ether component. The TTF unit prefers to occupy the central cavity of $CBPQT^{4+}$ ring much (>9:1) more so than does the DNP unit. (*B*) Stick diagrams of the solid-state structures of the degenerate and bistable [2]catenane obtained by X-ray crystallography. Note that only one—namely, that where the TTF unit is inside the cavity of the $CBPQT^{4+}$ ring and the DNP unit is outside—of the two translational isomers of the bistable [2]catenane has been characterized by X-ray crystallography in the solid state. In addition, note that the TTF unit inside the $CBPQT^{4+}$ cavity adopts the *trans* configuration. (*C*) and (*D*) Space-filling representations of the solid-state superstructures of the degenerate and bistable [2]catenanes. In both cases, the [2]catenane molecules form donor-acceptor stacks involving [$\pi\cdots\pi$] interactions between the outside π-electron-deficient bipyridium units and the alongside π-electron-rich units in the adjacent molecules.

The UV/Vis spectrum of $\mathbf{1}\cdot 4PF_6$, which was recorded in MeCN at 298 K (*SI Appendix*), reveals a CT absorption band centered on 800 nm, characteristic of co-conformations with the STTFS unit residing inside the $CBPQT^{4+}$ ring. In addition, however, a CT band centered on 540 nm, which arises when a DNP unit is located inside the $CBPQT^{4+}$ ring, is also observed for the other co-conformation. ^{1}H-^{1}H Gradient-selected Double-Quantum-Filtered Correlation Spectroscopy (^{1}H-^{1}H-g-DQF-COSY) was performed at 233 K on $\mathbf{1}\cdot 4PF_6$ in CD_3CN. The main proton resonances were assigned to these two sets of co-conformations (translational isomers) based on this COSY spectrum (*SI Appendix*). Both translational isomers ($\mathbf{1R}\cdot 4PF_6$ and $\mathbf{1G}\cdot 4PF_6$) of $\mathbf{1}\cdot 4PF_6$ were identified in CD_3CN at 233 K in a conventional ^{1}H NMR spectrum. Using specific DNP protons as probes, the ratio of $\mathbf{1R}\cdot 4PF_6$ to $\mathbf{1G}\cdot 4PF_6$ was ~1:1. The presence of approximately equimolar amounts of these two translational isomers in solution was also confirmed by cyclic voltammetry (CV) (*SI Appendix*). For $\mathbf{1}\cdot 4PF_6$, two oxidation potentials were recorded at +415 and +646 mV. The first peak at +415 mV arises from the first oxidation process ($STTFS \rightarrow STTFS^{+\bullet}$) of the alongside STTFS unit in $\mathbf{1G}\cdot 4PF_6$ and the peak at +646 mV is a combination of the first oxidation process for the inside STTFS and the second oxidation process ($STTFS^{+\bullet} \rightarrow STTFS^{2+}$) in both co-conformations. An attempt to follow the relaxation kinetics from $\mathbf{1G}^{4+}$ back to the equilibrium mixture of $\mathbf{1G}^{4+}$ and $\mathbf{1R}^{4+}$ by varying the CV scan rate revealed that the interconversion was too fast to be monitored at room temperature. By comparison with a previous investigation (34) on the bistable [2]catenane illustrated in Fig. 1*A*, the relaxation process must be associated with a free energy of activation ($\Delta G^{\ddagger}$ value) of less than 16 kcal mol^{-1}.

Both the degenerate (49, 50) and nondegenerate (27) [2]catenanes (Fig. 3*A*), which have been studied in the dim and distant past crystallized (Fig. 3*B*) as one-dimensional polar stacks (Fig. 3 *C* and *D*). The bistable [2]catenane (27) has only been isolated in crystalline form wherein the molecules that make up the polar stacks have their TTF units encircled by the $CBPQT^{4+}$ ring; i.e., it would appear to have undergone a crystallization-induced second-order transformation (51) insofar as the MSCC has not yet been obtained crystalline. We assumed that, during the crystallization of the GSCC, the small proportion of the MSCC at equilibrium presumably funnels through to the GSCC (Fig. 1*A*) during the kinetically controlled crystallization process. We hypothesized that, because the bistable [2]catenane $\mathbf{1}\cdot 4PF_6$ exists in solution as an approximately 1:1 mixture of the translational isomers (*SI Appendix*), it might undergo a first-order transformation (51); i.e., a solid mixture of crystals of the two translational isomers might be obtained reflecting the proportions present at equilibrium in solution. This situation is one we have not observed previously.

Slow vapor diffusion of $i\,Pr_2O$ into a MeCN solution of $\mathbf{1}\cdot 4PF_6$ at 298 K afforded a mixture (Fig. 4) of green and red crystals, both suitable for X-ray crystallography. The co-conformational assignments to the two isomers of $\mathbf{1}\cdot 4PF_6$ were made (Fig. 5*A*) following the isolation of a single red ($\mathbf{1R}\cdot 4PF_6$) and a single green ($\mathbf{1G}\cdot 4PF_6$) crystal from the mixture. It is worth noting here that the CT band for the TTF ⊂ $CBPQT^{4+}$ complex recorded in MeCN at 298 K is situated (27, 52) around 800–900 nm, an absorption that leads to a deep emerald colored solution. This emerald green color is also witnessed in the solid state for crystal (super) structures containing TTF units encircled by $CBPQT^{4+}$ rings; i.e., pseudorotaxanes, catenanes, and rotaxanes. The CT band for the DNP-TEG ⊂ $CBPQT^{4+}$ complex is situated (50,

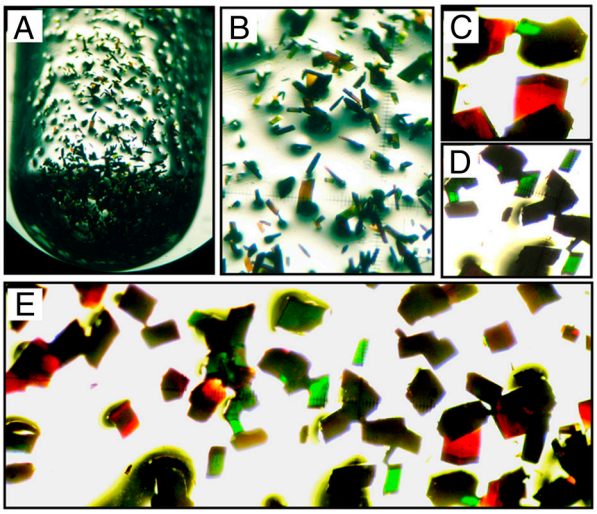

Fig. 4. Photographs of the single crystals grown by the vapor diffusion of $i\,Pr_2O$ into a solution of $\mathbf{1}\cdot 4PF_6$ in MeCN at 298 K. (*A*) Culture tube with two kinds of crystals growing on its surface. (*B*) Magnification of the previous photograph. (*C*)–(*E*) A selection of photographs taken at even higher magnification, showing the morphology of the two kinds of crystals, one red and the other green.

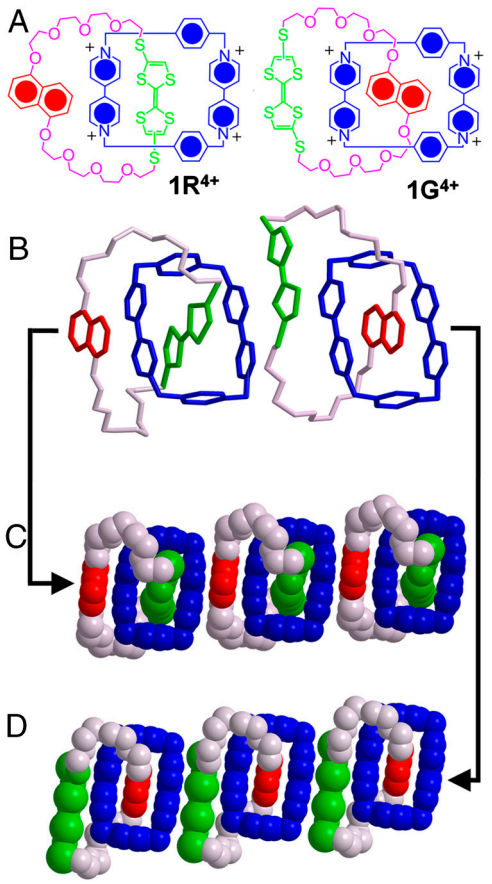

Fig. 5. (*A*) Structural formulas of the translational isomers $\mathbf{1R}^{4+}$ and $\mathbf{1G}^{4+}$ of the bistable [2]catenane $\mathbf{1}^{4+}$ containing DNP and STTFS units in the crown ether mechanically interlocked by the $CBPQT^{4+}$ ring. In $\mathbf{1R}^{4+}$, the STTFS unit is located inside the $CBPQT^{4+}$ ring, whereas, in $\mathbf{1G}^{4+}$, the encircled unit is a DNP one. (*B*) Stick diagrams of the solid-state structure of $\mathbf{1R}^{4+}$ and $\mathbf{1G}^{4+}$ determined by X-ray crystallography. Note that, although the inside STTFS unit in $\mathbf{1R}^{4+}$ assumes a *trans* configuration, the alongside STTFS unit in $\mathbf{1G}^{4+}$ adopts a *cis* configuration. (*C*) and (*D*) Space-filling representations of the solid-state superstructures of $\mathbf{1R}^{4+}$ and $\mathbf{1G}^{4+}$ highlighting their donor-acceptor stacks.

53) around 500–560 nm, resulting in a deep reddish-purple colored solution. Once again, this color is also expressed in the solid state where crystals containing DNP units encircled by $CBPQT^{4+}$ rings are also a deep reddish-purple color. In the light of these observations, it was surprising to us that the red crystal turned out to correspond to the co-conformation in which the STTFS unit is encircled by the $CBPQT^{4+}$ ring, whereas the green crystals correspond to the co-conformation in which the DNP unit is encircled by the tetracationic cyclophane. Remarkably, in the case of $\mathbf{1} \cdot 4PF_6$, the color of the crystal is derived principally from within the polar donor-acceptor stacks, rather than by the intramolecular CT interactions from within the [2]catenane itself; i.e., the solid-state (super)structure for $\mathbf{1R} \cdot 4PF_6$—the red crystals—corresponds to the co-conformation in which the STTFS units are encircled and bound by the $CBPQT^{4+}$ ring. When dissolved in CD_3COCD_3, the red crystal produces a characteristic emerald green colored solution at 190 K. Likewise, the solid-state (super) structure for $\mathbf{1G} \cdot 4PF_6$—the green crystals—corresponds to the co-conformation in which the DNP unit is encircled by the $CBPQT^{4+}$ ring.

The solid-state structures of $\mathbf{1R}^{4+}$ and $\mathbf{1G}^{4+}$ are shown in Fig. 5*B*. Both translational isomers are stabilized by the same $[\pi\cdots\pi]$, $[C-H\cdots\pi]$ and $[C-H\cdots O]$ interactions that have been shown to be present in the past in their degenerate (49, 50) and nondegenerate (27) counterparts (Fig. 3*B*). For $\mathbf{1R} \cdot 4PF_6$, the interplanar separations between the inside STTFS unit and the outside and inside bipyridinium units are 3.33 and 3.40 Å, respectively, whereas the plane-to-plane distance between the outside DNP unit and the inside bipyridinium unit is 3.47 Å. For $\mathbf{1G} \cdot 4PF_6$, the interplanar separations between the inside DNP unit and the outside and inside bipyridinium units are 3.58 and 3.20 Å, respectively, whereas the plane-to-plane distance between the outside STTFS unit and the inside bipyridinium unit is 3.56 Å. The packing (Fig. 5 *C* and *D*) in the solid state of the $\mathbf{1R}^{4+}$ and $\mathbf{1G}^{4+}$ tetracations (mean interplanar separations of 3.38 and 3.47 Å, respectively) is comprised of intermolecular donor–acceptor $[\pi\cdots\pi]$ interactions between the outside π-electron-deficient bipyridinium units and the alongside π-electron-rich DNP (in $\mathbf{1R}^{4+}$ polar stacks) and STTFS (in $\mathbf{1G}^{4+}$ polar stacks) units of adjacent bistable [2]catenane molecules, resulting in conventional polar donor-acceptor stacks. It is intriguing that $\mathbf{1}^{4+}$, which, in principle at least, is capable of forming three different types of polar donor–acceptor stacks—namely, (*i*) random stacks, (*ii*) alternating stacks, $\mathbf{1R} \cdot 4PF_6\cdots\mathbf{1G} \cdot 4PF_6\cdots\mathbf{1R} \cdot 4PF_6$, and (*iii*) homostacks, where $\mathbf{1R} \cdot 4PF_6\cdots\mathbf{1R} \cdot 4PF_6\cdots\mathbf{1R} \cdot 4PF_6$ stacks (Fig. 5*C*) constitute the red crystals, and where $\mathbf{1G} \cdot 4PF_6\cdots\mathbf{1G} \cdot 4PF_6\cdots\mathbf{1G} \cdot 4PF_6$ stacks (Fig. 5*D*) constitute the green crystals—opts to undergo a first-order transformation (51).

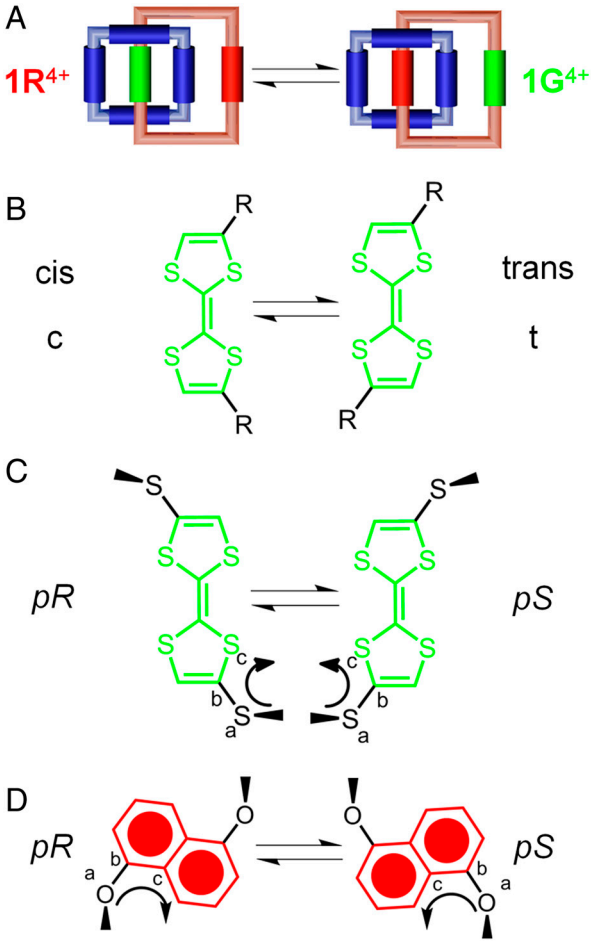

Fig. 6. (*A*) A graphical representation of the translational isomers $\mathbf{1R}^{4+}$ and $\mathbf{1G}^{4+}$ at equilibrium. (*B*) The interconversion between the *cis* and *trans* isomers of disubstituted TTF units. (*C*) The inversion of the plane of chirality between the (*pR*)- and (*pS*)- isomers for STTFS units. (*D*) The inversion of the plane of chirality between the (*pR*)- and (*pS*)-isomers for DNP units. In the case of both the STTFS and DNP units, the absolute chiralities have been defined as shown in (*C*) and (*D*).

When the red crystals of $\mathbf{1R} \cdot 4PF_6$ are dissolved in CD_3COCD_3 at 220 K, it is possible to follow the first-order decay by ^{1}H NMR spectroscopy (*SI Appendix*) of this translational isomer to an equilibrium mixture of the two isomers in which $\mathbf{1G} \cdot 4PF_6$ predominates. ^{1}H NMR spectra recorded at suitable time intervals during almost 17 h provided us with data, related to the changing proportions of $\mathbf{1R}^{4+}$ and $\mathbf{1G}^{4+}$ with time, from which a $\Delta G^{\ddagger}$ value of *ca.* 16 kcal mol^{-1} for the isomerism from $\mathbf{1R}^{4+}$ to $\mathbf{1G}^{4+}$ could be obtained. The $\Delta G^{\ddagger}$ value is very much in the expected (34) range for circumrotation of a crown ether containing tetrathiafulvalene and 1,5-dioxynaphthalene units through the cavity of the tetracationic cyclophane.

Conclusion

In stereochemical terms, the equilibration between $\mathbf{1R}^{4+}$ and $\mathbf{1G}^{4+}$ is far from being a simple and straightforward process. The complexity is brought about by $\mathbf{1}^{4+}$ having four sources of isomerism (Fig. 6), all of which are happening rapidly on the laboratory timescale and three of which are occurring at different rates on the ^{1}H NMR timescale. The *cis-trans* isomerism involving the STTFS units is a slow process on this timescale at room temperature. Whereas the circumrotation of the crown ether through the tetracationic cyclophane is sufficiently slow to give rise to two different sets of ^{1}H NMR signals at low temperature in solution, the other two processes, which involve the inversion of the planes of chirality (54) associated with the *trans*-STTFS and the DNP units, are occurring rapidly on the ^{1}H NMR timescale, even at 220 K.

The stereochemical situation as a whole is summarized in Fig. 7. There are a total of 12 isomers (six pairs of enantiomers) that are inverting (between enantiomeric forms) and interconverting (between isomers that are not enantiomers) rapidly on the laboratory timescale. We propose a hierarchy of isomerism that locates (*i*) the translational isomerism between $\mathbf{1R}^{4+}$ and $\mathbf{1G}^{4+}$ at the top of the tree, followed by (*ii*) the configurational isomerism between *cis* and *trans* STTFS units, and finally (*iii*) the conformational isomerism associated with the element of planar (*p*) chirality between (*pR*)- and (*pS*)-*trans*-STTFS units and likewise the conformational isomers associated with the element of planar (*p*) chirality between (*pR*)- and (*pS*)-DNP units. Thus, we classify the two isomers $\mathbf{1R}^{4+}$ and $\mathbf{1G}^{4+}$, which have crystallized out separately as, first and foremost, translational isomers (STTFS*i*/DNP*o* and STTFS*o*/DNP*i*), and then secondly, as configurational isomers (*c* and *t*) resulting from rotation about the C = C double bond in the middle of the STTFS unit, followed by the isomers, pR_{STTFS} and pS_{STTFS}, created as a result of the planar chirality associated with the STTFS unit and, finally, the isomers, pR_{DNP} and pS_{DNP}, created as a consequence of the planar chirality associated with the DNP unit. From this dynamic pool of 12 isomers, two pairs of enantiomers—namely (c-pS_{DNP_i}/c-pR_{DNP_i} and t-pR_{STTFS_i}-pR_{DNP_o}/t-pS_{STTFS_i}-pS_{DNP_o})—crystallize out by a first-order transformation event.

In the event, $\mathbf{1R}^{4+}$ and $\mathbf{1G}^{4+}$ are simultaneously translational, configurational, and conformational isomers in a situation where isomerism is a highly dynamic phenomenon. Put another way, this research has established the concept of dynamic isomerism in a bistable [2]catenane containing four sources of isomerism, which are equilibrating rapidly with one another in solution at room temperature. One can speculate that such a molecule should be highly adaptive to its surroundings, solution or otherwise, chiral or achiral. It is a molecule that "wears a coat of many colors," depending on its environment in solution from which it can produce spontaneously coats of two different colors on selective crystallization under the appropriate conditions.

Materials and Methods

Synthesis and Characterization of the Bistable [2]Catenane 1 · 4PF$_6$. A mixture of 4,4′-bis(bromomethyl)benzene (105 mg, 0.40 mmol), the macrocycle **4** (100 mg, 0.13 mmol), and 1,1′-[1,4-phenylenebis(methylene)]-bis(4,4′-bipyridinium) bis(hexafluoro phospate) (55) (285 mg, 0.40 mmol) was dissolved in N-N-dimethylformamide (10 mL). The reaction mixture was subjected to

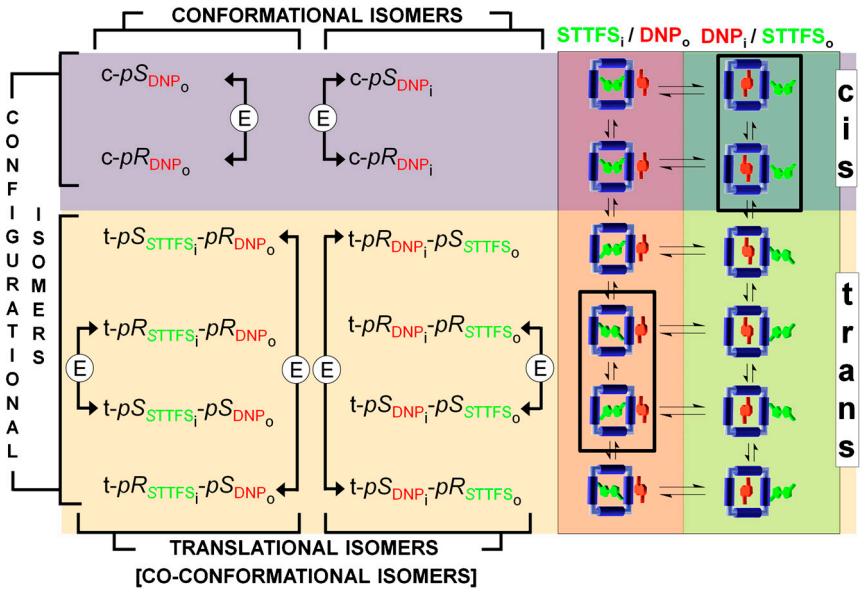

Fig. 7. A chart and supporting graphical display showing the dynamic interplay between translational, configurational and conformational isomerism in the bistable [2]catenane $\mathbf{1}^{4+}$ molecule that experiences (*i*) *cis-trans* isomerism of its STTFS units, (*ii*) translational isomerism depending upon whether its STTFS or DNP unit is located inside the cavity of the CBPQT^{4+} ring, and (*iii*,*iv*) two conformational processes involving the inversion of the planes of chirality associated with both its STTFS and DNP units. The configurational isomerism is denoted by "c" for the *cis*-isomers and "t" for the *trans*-isomers. The subscripts "i" and "o" following the acronyms STTFS and DNP indicate whether these units are inside or outside the CBPQT^{4+} ring in the translational isomers. The dynamic planar chirality is designated, according to the Cahn–Ingold–Prelog rules, as (*pR*) or (*pS*). See Fig. 6. This dynamic stereochemistry yields 12 possible isomers in solution. The designations of their structures to stereochemical descriptors indicates that there are actually six pairs of enantiomers. The two pairs of enantiomers that have yielded single crystals simultaneously from crystal growing experiments, and for which the solid-state structures have been solved by X-ray crystallography, are surrounded by two black rectangles. Note that the equilibrium arrows do not necessarily represent a specific inversion or interconversion process. E identifies the six pairs of enantiomers.

15 kbar in an ultra high pressure reaction chamber at room temperature for 3 d, the resulting green solution was subjected to column chromatography [SiO_2 : Me_2CO/NH_4PF_6 (100 : 1, v/w)]. The green band was collected and most of the solvent was removed under reduced pressure, followed by the addition of H_2O (10 mL). The precipitate was collected by filtration and washed with H_2O (3×20 mL), to give the pure product $\mathbf{1} \cdot 4PF_6$ as a green solid (132 mg, 55%). ^1H NMR (CD_3CN, 600 MHz, 233 K, ppm): $\delta = 2.29$ (d, $J = 8.0$ Hz, ~1H), 2.76–2.82 (m, ~2H), 2.91–3.00 (m, ~2H), 3.40–4.30 (m, 28H), 5.54–5.94 (m, 10H), 6.17 (t, $J = 7.9$ Hz, ~1H), 6.20–6.25 (m, 1H), 6.43 (d, $J = 7.6$ Hz, ~0.95H), 6.54 (d, $J = 7.7$ Hz, ~0.05H), 7.14–8.09 (m, 18H), 8.58–9.01 (m, 8H). HR MS (ESI): Calculated for $C_{68}H_{72}F_{24}N_4O_8P_4S_6$ $m/z = 1699.2594$ $[M - PF_6]^+$, 777.1474 $[M - 2PF_6]^{2+}$, found $m/z = 1699.2559$ $[M - PF_6]^+$, 777.1475 $[M - 2PF_6]^{2+}$.

Crystallization of the Bistable [2]Catenane $\mathbf{1} \cdot 4PF_6$. The green solid was dissolved in MeCN in a small test tube and was subjected to slow (~2 weeks) vapor diffusion with $i\,Pr_2\,O$ contained in a larger sealed vial. Under these crystallization conditions, batches of both red and green single crystals formed on the sides of the test tube. With the aid of a stereomicroscope, the crystals were detached with considerable care from the sides of the test tube using a dissecting needle. The freed crystals were transferred into a glass Petri dish (60×15 mm), which was covered to prevent solvent evaporation. Using tweezers and a stereomicroscope, the red and green crystals were separated mechanically and placed in separate vials. Signal crystals, suitable for X-ray analysis were investigated to determine (Fig. 5) their solid-state structures. The data were corrected for Lorentz and polarization effects.

ACKNOWLEDGMENTS. This material is based upon work supported by the National Science Foundation under CHE-0924620. The authors also wish to thank and acknowledge the support from the Air Force Office of Scientific Research under the Multidisciplinary Research Program of the University Research Initiative (MURI), Award FA9550-07-1-0534 entitled "Bioinspired Supramolecular Enzymatic Systems."

1. Stoddart JF, Colquhoun HM (2008) Big and little Meccano. *Tetrahedron* 64:8231–8263.
2. Stoddart JF (2009) The chemistry of the mechanical bond. *Chem Soc Rev* 38:1802–1820.
3. Kay ER, Leigh DA, Zerbetto F (2007) Synthetic molecular motors and mechanical machines. *Angew Chem Int Ed Engl* 46:72–191.
4. Tseng HR, et al. (2003) Dynamic chirality: Keen selection in the face of stereochemical diversity in mechanically bonded compounds. *Chem Eur J* 9:543–556.
5. Vignon SA, Stoddart JF (2005) Exploring dynamics and stereochemistry in mechanically interlocked compounds. *Collect Czech Chem C* 70:1493–1576.
6. Schill G, Rissler K, Fritz H, Vetter W (1981) Synthesis, isolation, and identification of translationally isomeric [3]catenanes. *Angew Chem Int Ed Engl* 20:187–189.
7. Raymo FM, Houk KN, Stoddart JF (1998) Origins of selectivity in molecular and supramolecular entities. Solvent and electrostatic control of the translational isomerism in [2]catenanes. *J Org Chem* 63:6523–6528.
8. Grabuleda X, Jaime C (1998) Molecular shuttles. A computational study (MM and MD) on the translational isomerism in some [2]rotaxanes. *J Org Chem* 63:9635–9643.
9. Gunter MJ, Farquhar SM, Jeynes TP (2003) Translational isomerism and dynamics in multi-hydroquinone derived porphyrin [2]- and[3]catenanes. *Org Biomol Chem* 1:4097–4112.
10. Fallon GD, Lee MAP, Langford SJ, Nichols PJ (2004) Unusual solid-state behavior in a neutral [2]catenane bearing a hydrolyzable component. *Org Lett* 6:655–658.
11. Leigh DA, et al. (2005) Patterning through controlled submolecular motion: rotaxane-based switches and logic gates that function in solution and polymer films. *Angew Chem Int Ed Engl* 44:3062–3067.
12. Marlin DS, Cabrera DG, Leigh DA, Slawin AMZ (2006) Complexation-induced translational isomerism: Shuttling through stepwise competitive binding. *Angew Chem Int Ed Engl* 45:77–83.
13. Lin CF, Lai CC, Liu YH, Peng SM, Chiu SH (2007) Use of anions to allow translational isomerism of a [2]rotaxane. *Chem Eur J* 13:4350–4355.
14. Fioravanti G, et al. (2008) Three state redox-active molecular shuttle that switches in solution and on a surface. *J Am Chem Soc* 130:2593–2601.
15. Schill G (1971) *Catenanes, Rotaxanes and Knots* (Academic, New York).
16. Sauvage JP, Dietrich-Buchecker CO, eds. (1999) *Molecular Catenanes, Rotaxanes and Knots* (Wiley-VCH, Weinheim).
17. Fyfe MCT, et al. (1997) Anion-assisted self-assembly. *Angew Chem Int Ed Engl* 36:2068–2070.
18. Steuerman DW, et al. (2004) Molecular mechanical switch-based solid-state electrochromic devices. *Angew Chem Int Ed Engl* 43:6486–6491.
19. Dichtel WR, Heath JR, Stoddart JF (2007) Designing bistable [2]rotaxanes for molecular electronic devices. *Philos Tr R Soc S-A* 365:1607–1625.
20. Eliel EL, Wilen SH (1994) *Stereochemistry of Organic Compounds* (Wiley-Interscience, New York).
21. Gross LC, Klyne W (1976) Rules for the nomenclature of organic chemistry. Section E: Stereochemistry. *Pure Appl Chem* 45:11–30.
22. Sutherland IO (1971) Investigation of the kinetics of conformational changes by nuclear magnetic resonance spectroscopy. *Ann R NMR S* 4:71–235.
23. Eliel EL (1965) Conformational analysis in mobile cyclohexane systems. *Angew Chem Int Ed Engl* 4:761–774.
24. Franklin NC, Feltkamp H (1965) Conformational analysis of cyclohexane derivatives by nuclear magnetic resonance spectroscopy. *Angew Chem Int Ed Engl* 4:774–783.
25. Jensen FR, Bushwell CH (1969) Separation of conformers. 2. Axial and equatorial isomers of chlorocyclohexane and trideuteriomethoxycyclohexane. *J Am Chem Soc* 91:3223–3225.
26. Hoorfar A, Ollis WD, Price JA, Stephanatou JS, Stoddart JF (1982) Conformational behaviour of medium sized rings. Part 1. Dianthranilides and trianthranilides. *J Chem Soc Perk T 1* 1637–1648.
27. Asakawa M, et al. (1998) A chemically and electrochemically switchable [2]catenane incorporating a tetrathiafulvalene unit. *Angew Chem Int Ed Engl* 37:333–337.
28. Tseng HR, Vignon SA, Stoddart JF (2003) Toward chemically controlled nanoscale molecular machinery. *Angew Chem Int Ed Engl* 42:1491–1495.
29. Tseng HR, et al. (2004) Redox-controllable amphiphilic [2]rotaxanes. *Chem Eur J* 10:155–172.
30. Jeppesen JO, Nygaard S, Vignon SA, Stoddart JF (2005) Honing up a genre of amphiphilic bistable [2]rotaxanes for device settings. *Eur J Org Chem* 196–220.
31. Collier CP, et al. (2000) A [2]catenane-based solid state electronically reconfigurable switch. *Science* 289:1172–1175.
32. Collier CP, et al. (2001) Molecular-based electronically switchable tunnel junction devices. *J Am Chem Soc* 123:12632–12641.
33. Olson MA, et al. (2009) Thermodynamic forecasting of mechanically interlocked switches. *Org Biomol Chem* 7:4391–4405.
34. Choi JW, et al. (2006) Ground-state equilibrium thermodynamics and switching kinetics of bistable [2]rotaxanes switched in solution, polymer gels, and molecular electronic devices. *Chem Eur J* 12:261–279.
35. Jeppesen JO, Perkins J, Becher J, Stoddart JF (2001) Slow shuttling in an amphiphilic bistable [2]rotaxane incorporating a tetrathiafulvalene unit. *Angew Chem Int Ed Engl* 40:1216–1221.
36. Jeppesen JO, et al. (2003) Amphiphilic bistable rotaxanes. *Chem Eur J* 9:2982–3007.
37. Luo Y, et al. (2002) Two-dimensional molecular electronics circuits. *Chemphyschem* 3:519–525.
38. Green JE, et al. (2007) A 160-kilobit molecular electronic memory patterned at 10^{11} bits per square centimetre. *Nature* 445:414–417.
39. Klajn R, et al. (2009) Metal nanoparticles functionalized with molecular and supramolecular switches. *J Am Chem Soc* 131:4233–4235.
40. Coskun A, et al. (2010) Molecular-mechanical switching at the nanoparticle-solvent interface: Practice and theory. *J Am Chem Soc* 132:4310–4320.
41. Nguyen TD, et al. (2005) A reversible molecular valve. *Proc Natl Acad Sci USA* 102:10029–10034.
42. Cotí KK, et al. (2009) Mechanised nanoparticles for drug delivery. *Nanoscale* 1:16–39.
43. Jia CY, Zhang DQ, Xu W, Zhu DB (2001) A new approach to 4-alkylthio-1,3-dithiole-2-thione: An unusual reaction of a zinc complex of 1,3-dithole-2-thione-4,5-dithiolate. *Org Lett* 3:1941–1944.
44. Guo XF, et al. (2003) Donor-acceptor-donor triads incorporating tetrathiafulvalene and perylene diimide units: Synthesis, electrochemical and spectroscopic studies. *Tetrahedron* 59:4843–4850.
45. Ashton PR, et al. (1996) Bis[2]catenanes and a bis[2]rotaxane—Model compounds for polymers with mechanically interlocked components. *Chem Eur J* 2:31–44.
46. Benítez D, Tkatchouk E, Yoon I, Stoddart JF, Goddard WA, III (2008) Experimentally-based recommendations of density functionals for predicting properties in mechanically interlocked molecules. *J Am Chem Soc* 130:14928–14929.
47. Zhao Y, Truhlar DG (2006) Density functional for spectroscopy: No long-range self-interaction error, good performance for Rydberg and charge-transfer states, and better performance on average than B3LYP for ground states. *J Phys Chem A* 110:13126–13130.
48. Reed AE, Weinstock RB, Weinhold F (1985) Natural population analysis. *J Chem Phys* 83:735–746.
49. Ashton PR, et al. (1989) A [2]catenane made to order. *Angew Chem Int Ed Engl* 28:1396–1399.
50. Ashton PR, et al. (1991) The self-assembly of a highly ordered [2]catenane. *J Chem Soc Chem Commun* 634–639.
51. Jacques J, Collet A, Wilen SH (1981) *Enantiomers, Racemates, and Resolution* (Wiley, New York), pp 370–371.
52. Philp D, Slawin AMZ, Spencer N, Stoddart JF, Williams DJ (1991) The complexation of tetrathiafulvalene by cyclobis(paraquat-*p*-phenylene). *J Chem Soc Chem Commun* 1584–1586.
53. Reddington MV, et al. (1991) Towards a molecular abacus. *J Chem Soc Chem Commun* 630–634.
54. Cahn RS, Ingold CK, Prelog V (1966) Specification of molecular chirality. *Angew Chem Int Ed Engl* 5:385–415.
55. Anelli PL, et al. (1992) [2]Rotaxanes and a [2]catenane made to order. *J Am Chem Soc* 114:193–218.